HHS Public Access

Author manuscript

J Mol Cell Cardiol. Author manuscript; available in PMC 2024 December 14.

Published in final edited form as:

J Mol Cell Cardiol. 2023 October ; 183: 22–26. doi:10.1016/j.yjmcc.2023.08.004.

Tnni3k Influences Cardiomyocyte S-Phase Activity and Proliferation

Alexandra L. Purdy[1,*], **Samantha K. Swift**[1,*], **Henry M. Sucov, PhD**[2], **Michaela Patterson, PhD**[1,3]

[1]Department of Cell Biology, Neurobiology, and Anatomy, Medical College of Wisconsin, Milwaukee, Wisconsin

[2]Department of Regenerative Medicine and Cell Biology, Medical University of South Carolina, Charleston, South Carolina

[3]Cardiovascular Center, Medical College of Wisconsin, Milwaukee, Wisconsin

Abstract

Cardiomyocyte proliferation is a difficult phenomenon to capture and prove. Here we employ a retrospective analysis of single cell ventricular suspensions to definitively identify cardiomyocytes that have completed cell division. Through this analysis we determined that the capacity of cardiomyocytes to re-enter the cell cycle and complete cell division after injury are separate and variable traits. Further, we provide evidence that *Tnni3k* definitively influences both early and final stages of the cell cycle.

Graphical Abstract

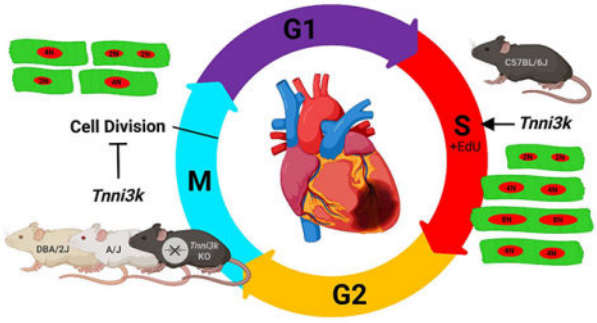

Corresponding Author: Michaela Patterson, Ph.D., Medical College of Wisconsin, 8701 Watertown Plank Road, MEB4575, Milwaukee, WI 53226, mpatterson@mcw.edu.

*These authors contributed equally to this work

Declaration of Competing Interests

The authors declare no conflicts of interest.

Keywords

Cardiomyocyte; polyploidization; proliferation; heart regeneration

1. Introduction

Demonstration of cardiomyocyte (CM) proliferation in the adult mammalian heart is technically challenging. Most adult CMs are polyploid, having a total chromosomal content of 4N, 8N, or higher, where N is the haploid genome. Polyploidization occurs via endomitosis, which is defined by cell cycle re-entry with S-phase DNA replication and failure to complete mitosis or cell division. After injury, such as myocardial infarction, CM cell cycle activation can either result in further polyploidization or proliferation if cell division is completed. In the latter scenario two new daughter cells are generated. Typical cell cycle markers of S-phase, mitosis, and even cytokinesis are unable to decipher these two scenarios [1]. Thus, there is longstanding interest in establishing methods that can distinguish the two outcomes, while also identifying the mechanisms that specifically potentiate proliferation.

In our prior work [2], we demonstrated that the diploid:polyploid ratio of ventricular CMs in the uninjured adult heart varies considerably across inbred mouse strains. This observation is explained by natural genetic variants, i.e., polymorphisms, that differ across strains. Using mononuclear CM frequency as the basis for a genome-wide association analysis, we identified *Tnni3k* as one gene that influences CM ploidy. There is a natural splice site polymorphism in the *Tnni3k* gene carried by A/J, DBA/2J, and many other mouse strains that results in a severely hypomorphic, essentially null, allele [3]. The functional *Tnni3k* gene, as for example in C57BL/6J, is associated with having fewer diploid CMs, whereas homozygosity of the natural hypomorphic allele is associated with having more diploid CMs. We confirmed this as a causal relationship by demonstrating that engineered *Tnni3k* null mice, established and maintained on an isogenic C57BL/6J background, have a several-fold increase in diploid CM content [2]. It is clear however that a multitude of additional variants exist across inbred mouse lines, and every inbred strain carries its own unique set of polymorphisms that both positively and negatively influence the final diploid level.

Genes that influence the natural diploid CM level of the uninjured heart might similarly influence the degree of CM cell cycle completion after injury. In our past work, we took an indirect strategy to address this for *Tnni3k*. To distinguish proliferation from further polyploidization post-infarction, we separately assessed nucleation and nuclear ploidy after EdU incorporation to then calculate total cellular ploidy of EdU-positive cycling CMs. The premise of this retrospective approach is that an EdU-positive and diploid CM must have undergone S-phase DNA replication and completed cell division, i.e., proliferated. We concluded that CMs from A/J mice and from C57BL/6J mice with engineered *Tnni3k* knockout were more competent to complete cell division [2].

A recent study by Reuter et al. [4] also identified *Tnni3k*, but instead from an F2 genome mapping analysis following assessment of CM S-phase activity post-infarction.

They subsequently assessed CM cell division in C57Bl6/NCrl (functional *Tnni3k*) versus DBA/2J (*Tnni3k* null) mice but observed no CM proliferation in either strain, coming to the conclusion that *Tnni3k* does not affect CM proliferation. This conclusion, which may appear in conflict with our original results, was based only on the comparison of these two strains. Thus here, we employed a novel and improved methodology to definitively assess the effect of *Tnni3k* on the capacity of CMs to divide.

2. Materials and Methods

2.1 Mice

All experiments involving animals were performed in accordance with the local Institutional Animal Care and Use Committee. A/J (JAX stock #000646), C57Bl/6J (JAX stock #000664), and DBA/2J (JAX stock #000671) mice were purchased from Jackson Laboratory, Bar Harbor, Maine. *Tnni3k* global knockout mice were generated as described in [2] and maintained for more than 10 generations on a C57Bl/6J background. *Tnni3k* heterozygotes were bred inhouse to generate homozygous wildtype (+/+) and homozygous knockout (−/−) littermates used in the described studies.

2.2 Myocardial infarction and EdU administration

While maintained under 2–4% isoflurane, the heart was extruded from the thoracic cavity via the 4th intercostal space and the left anterior descending artery was permanently ligated with a 6–0 prolene suture [2, 5, 6]. For continuous labeling of cycling CMs, ALZET Osmotic Pumps (ALZET, 1007D) carrying 2.5mg of EdU were implanted subcutaneously between scapula on day 3 post-infarction, removed on day 10, and followed by a 48-hour chase period (Fig. 1A).

2.3 Single cell ventricular suspensions

Hearts were extracted, hung on a Langendorff apparatus, and digested as described in [6]. Following perfusion, ventricular tissue was diced with scissors, triturated with a wide bore pipette in 4°C Kruftbruhe (KB) solution, and fixed for 10 minutes by adding an equal volume of 8% PFA. Following fixation, cell suspensions were spun down at 300G for 2 minutes and resuspended in Phosphate Buffered Saline.

2.4 Immunostaining of single cell suspensions

Fixed single cell suspensions were stained and prepared as described in [6]. Additional primary antibodies include rabbit anti-Connexin43 (CX43), 1:500, Abcam ab11370; and goat anti-NKX2–5, 1:250, abcam ab106923.

2.5 Ploidy analysis and assessment of cell division

Ploidy analysis and quantification of EdU-positive CMs was performed as described in [6]. Briefly, stained slides were manually scanned by eye in their entirety on a Nikon Eclipse 80i fluorescent microscope with a 20x objective for all EdU-positive CMs. The total number of EdU-positive CMs on each quantified slide was noted. EdU-positive CMs were then assessed for their nucleation status (i.e. mono-, bi-, tri-, or tetranucleated). Subsequently,

images of the EdU-positive CMs captured using a PCO Panda camera were analyzed using NIS Elements software for the sum DAPI fluorescent intensity of each nucleus. To estimate total DNA content, the raw values were normalized to a known 2N nucleus as described in [6]. Cutoffs for ploidy classes were determined by EdU-negative CMs and break points between populations, as is done by flow cytometry. Normalized values ranging from 1.2–2.8 were deemed 2N, 3.2–5.8 4N, 6.0–11.8 8N, and >12.0 16N. The two metrics, nucleation and single nucleus ploidy, were combined to determine the frequency of mononuclear diploid EdU-positive CMs represented as a percent of the total EdU-positive CMs.

2.6 Immunofluorescence on tissue sections

Hearts were dissected, washed in KB solution until no longer beating, and hung on a Langendorff apparatus. Hearts were perfused with 5mLs of calcium-free Tyrodes to flush out any remaining blood, followed by 5mLs of 4% PFA before being further fixed in 4% PFA overnight at 4°C. Processed tissue was embedded in paraffin wax, sectioned on a Thermo Microm HM355S microtome at 4μm from apex to outflow track, and collected onto slides for staining. Tissue sections were deparaffinized, rehydrated, and heated at 100°C in Sodium Citrate buffer with 0.1% Triton-X-100 and .05% Tween-20, pH6.0 for 30 minutes. Slides were blocked with 5% normal donkey serum and 5% bovine serum albumin before addition of primary antibodies (goat anti-NKX2–5, 1:250, abcam ab106923; rabbit anti-AURKB, 1:100, abcam ab2254; mouse anti-cTnT, 1:500, abcam ab8295). Following primary antibody incubation overnight at 4°C the remainder of the stain followed the protocol detailed in [6].

2.7 Statistics

For analyses comparing three conditions, statistical significance was calculated by a one-way ANOVA and post-hoc TukeyHSD pairwise comparisons. For analyses comparing two conditions, statistical significance was calculated by a Student t-test with and without Welch's correction for unequal variance as indicated in the figure legend.

3. Results and Discussion

In the current study (Fig. 1A), our single-cell methodology assesses both nucleation and ploidy from the same EdU-positive cell. As before, an EdU-positive CM must have completed cell division if it is both mononuclear and diploid (Fig. 1B–E). In accordance with Reuter et al. [4], C57BL/6J mice had ~14-fold more total EdU-positive CMs compared to either A/J or DBA/2J (Fig. 1F). However, the increased DNA synthesis in C57BL/6J mice was likely further polyploidization, as no EdU-positive mononuclear diploid CMs were found (Fig. 1G). Conversely, we observed a substantial level (13.7%) of EdU-positive, mononuclear diploid CMs in A/J hearts but many fewer in DBA/2J, both of which are *Tnni3k* hypomorphs (Fig. 1G). An artifactual explanation for this outcome is unlikely as >98% of CMs analyzed in our hands by this method retain markers of intercalated discs (e.g., CX43) at both ends and express CM nuclear markers (e.g., NKX2–5, Supp Fig. 1). The ability of CMs from select strains to initiate cytokinesis was confirmed by an independent assessment examining AURKB staining in tissue sections (Fig. 1H–I).

To directly test the role of *Tnni3k* in cell division after infarction, we performed the same single-cell analysis on C57BL/6J-inbred *Tnni3k* engineered knockouts (−/−) compared to wildtype (+/+) littermates. Reduced S-phase activity (Fig. 1J) accompanied by enhanced cell division (Fig. 1K) were both identified in *Tnni3k* knockouts. This outcome is consistent with observations in normal postnatal development where absence of *Tnni3k* enhances completion of cell division [6], and in zebrafish where overexpression of mouse *Tnni3k* induced polyploidization [2], which cannot be explained solely by activation of S-phase.

Reuter et al. [4] focused on the observation that *Tnni3k* drives enhanced S-phase activity when the entire ventricular myocardium is considered, a conclusion with which we now agree. Our major conclusion in Patterson et al. [2] was that loss of *Tnni3k* potentiated CM cell cycle completion, which we were able to demonstrate using unambiguous methodology in this present study. For functional *Tnni3k* to have both properties (enhancing S-phase while also inhibiting proliferation) need not be in conflict, as this is exactly what is necessary to drive endomitosis [7].

The primary discrepancy between the two labs is whether *Tnni3k* influences CM cell division following injury. Reuter et al. [4] also tested proliferation by a single-cell suspension method but only compared DBA/2J versus C57BL/6NCrl. We agree, cell division is not detectable in C57BL/6 and is rare in DBA/2J (Fig. 1G). Critically, these two strains differ by much more than only *Tnni3k*. In a fully controlled isogenic background, ~3% of *Tnni3k* null CMs that enter the cell cycle complete cell division (Fig. 1K), and this is >13% in A/J mice (Fig. 1G). Both numbers are reduced from what we originally reported [2], which is explained by the improved methodology employed in this study. These results definitively test and confirm that *Tnni3k* regulates CM cell division. Notably, it is only partially responsible for the full phenotypic variation observed across strains. *Tnni3k*, given its expression specificity to CMs, is likely to be an intrinsic mechanism controlling CM cell division, however additional non-myocyte contributions may add further complexity between strains. Thus, both additional genetic and cellular complexities are likely contributing to the total observed variation.

Although the level of proliferation in DBA/2J mice in our analysis was low, it was above zero as claimed by Reuter et al. One explanation for this inconsistency could stem from their use of an *Myh6-nLacZ* transgene to identify CM nuclei. Several studies suggest that CMs undergoing dedifferentiation and/or proliferation switch expression from *Myh6* to *Myh7* [[8, 9], and discussed in [1]]. Thus, the reporter used by Reuter et al. could miss the dividing CM population of interest. We acknowledge the necessity of utilizing a nuclear marker for quantifying CM cell cycle in tissue sections, however misidentifying CMs in single cell preparations is not an issue.

The method we utilize here has limitations but is arguably the best currently available for detecting completion of cell division. Advantages include an irrefutable output (EdU-positive, mononuclear, and diploid) and universal applicability. On the negative, conclusions of proliferation are drawn retrospectively and the challenge of digesting a fibrotic heart likely results in undercounting of proliferative events, which were recently reported to occur preferentially around the infarction [10]. Fluorescence intensity of DAPI approximates

total DNA content within a nucleus and cannot address more specific anomalies like incorrect chromosomal segregation resulting in aneuploidy. Finally, we cannot rule out "false negatives", where cell division may have taken place but resulted in a final ploidy content greater than 2N, as has been described in the hepatocyte field [11]. While our method likely underestimates the frequency of cell division events, our comparison of knockouts to isogenic controls provides unmistakable evidence that *Tnni3k* influences CM proliferation.

Supplementary Material

Refer to Web version on PubMed Central for supplementary material.

Acknowledgements

Schematics were created using *BioRender*.

Sources of funding

This work was supported by the American Heart Association, 18CDA34110240 awarded to M.P., and the National Institutes of Health: F31HL162468 awarded to S.K.S, R01HL144938 award to H.M.S., and R01HL155085 awarded to M.P. A.L.P is also supported on a National Institutes of Health T32HL007852 training grant.

Abbreviations

CM	Cardiomyocyte
EdU	5-Ethynyl-2′-deoxyuridine
Aurkb	Aurora Kinase B
CX43	Connexin 43

References

1. Auchampach J, et al. , Measuring cardiomyocyte cell-cycle activity and proliferation in the age of heart regeneration. Am J Physiol Heart Circ Physiol, 2022. 322(4): p. H579–H596. [PubMed: 35179974]
2. Patterson M, et al. , Frequency of mononuclear diploid cardiomyocytes underlies natural variation in heart regeneration. Nat Genet, 2017.
3. Wheeler FC, et al. , Tnni3k modifies disease progression in murine models of cardiomyopathy. PLoS Genet, 2009. 5(9): p. e1000647. [PubMed: 19763165]
4. Reuter SP, et al. , Cardiac Troponin I-interacting Kinase Impacts Cardiomyocyte S-phase Activity But Not Cardiomyocyte Proliferation. Circulation, 2022.
5. Gao E, et al. , A novel and efficient model of coronary artery ligation and myocardial infarction in the mouse. Circ Res, 2010. 107(12): p. 1445–53. [PubMed: 20966393]
6. Swift SK, et al. , Cardiomyocyte ploidy is dynamic during postnatal development and varies across genetic backgrounds. Development, 2023. 150(7).
7. Ovrebo JI and Edgar BA, Polyploidy in tissue homeostasis and regeneration. Development, 2018. 145(14).
8. Zhang Y, et al. , Single-cell imaging and transcriptomic analyses of endogenous cardiomyocyte dedifferentiation and cycling. Cell Discov, 2019. 5: p. 30. [PubMed: 31231540]

9. Cui M, et al. , Dynamic Transcriptional Responses to Injury of Regenerative and Non-regenerative Cardiomyocytes Revealed by Single-Nucleus RNA Sequencing. Dev Cell, 2020. 55(5): p. 665–667. [PubMed: 33290696]

10. Liu X, et al. , Cell proliferation fate mapping reveals regional cardiomyocyte cell-cycle activity in subendocardial muscle of left ventricle. Nat Commun, 2021. 12(1): p. 5784. [PubMed: 34599161]

11. Miyaoka Y, et al. , Hypertrophy and unconventional cell division of hepatocytes underlie liver regeneration. Curr Biol, 2012. 22(13): p. 1166–75. [PubMed: 22658593]

Highlights

- CM ploidy in the naïve adult myocardium and cell cycle activity in response to injury are highly variable traits.
- Some of the genetic drivers that regulate CM ploidy also in turn influence cell cycle activation and completion after injury.
- *Tnni3k* influences both S-phase activity and completion of the cell cycle.

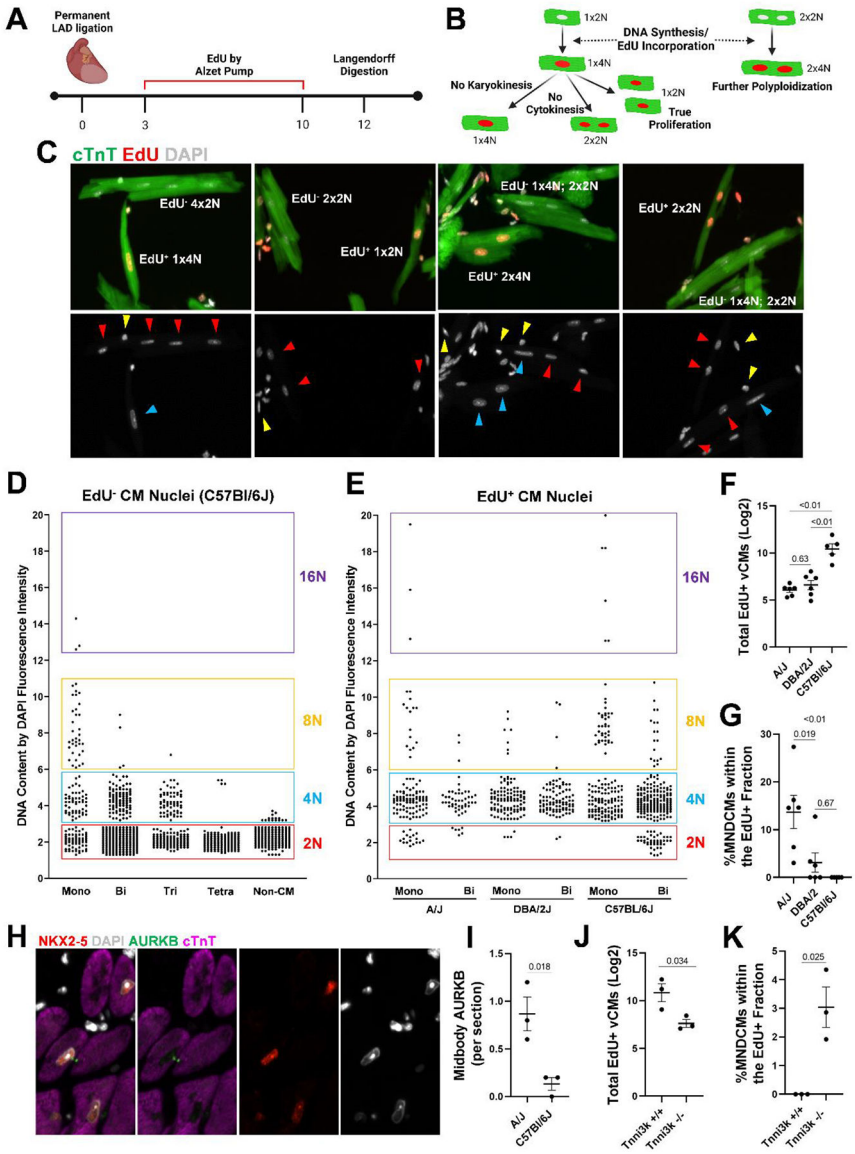

Figure 1. Definitive proliferation in adult CMs after MI.

(A) Schematic of the experimental time course. Experimental myocardial infarction (MI) was performed on 8-week-old female A/J (N=6), DBA/2J (N=6), and C57BL/6J (N=5) mice, or 8-week-old male and female global *Tnni3k* knockout (N=3) and wild-type littermate (N=3) mice, by permanent ligation of the left anterior descending (LAD) artery. On the 3rd day after MI, Alzet osmotic pumps containing EdU (25mg/mL) were implanted underneath the dorsal skin. Pumps were removed on the 10th day post-MI, followed by euthanasia and collection of hearts for Langendorff digestion on the 12th day post-MI, allowing for a chase period for CMs to complete division. **(B)** Schematic illustrating EdU-labeling events. CMs that are mononuclear, diploid and EdU-positive are considered products of completed cell division, i.e., “True Proliferation”. Other scenarios are detailed in the schematic. **(C)** Example fluorescent images of CMs stained for cardiac Troponin T (cTnT, green), EdU (red), and DAPI (grayscale). Upper panels are merged images; lower

panels are DAPI-channel only used to assess ploidy by sum DAPI fluorescent intensity. Cells are labeled as Edu-negative (EdU^-) or EdU-positive (EdU^+) and with the nuclear and ploidy classifications. In lower DAPI-only panel, red arrowheads point to 2N nuclei, blue arrowheads point to 4N nuclei, yellow arrowheads indicate non-CMs. **(D-E)** Example ploidy plots from EdU^- CMs from a single C57BL/6J mouse (D), and EdU^+ CMs from 3 inbred strains (E) 12 days post-MI as assessed by the summation of DAPI fluorescence intensity of a single nucleus and normalized to known diploid (2N) nuclei from tri- and tetranucleated CMs from the same picture. Each dot is an individually sampled nucleus from either a mononucleated (Mono), binucleated (Bi), trinucleated (Tri), tetranucleated (Tetra), or non-CM, as indicated. Boxes indicate the "gates" for the 2N (red), 4N (blue), 8N (yellow), and 16N (purple) populations. **(F)** Total EdU^+ CMs identified in single-cell suspensions of ventricular tissue post-MI across three inbred strains (A/J, DBA/2J, and C57BL/6J), N mentioned above in (A). Data represented in Log2 scale. P-values calculated by one-way ANOVA (P = 0.0022) with post-hoc Tukey HSD pairwise comparisons indicated on graph. **(G)** Percent of EdU^+ CMs from post-MI single cell suspensions that were specifically mononuclear and diploid represented as a percent of the total EdU^+ CM population, indicating completion of cell division as depicted in (B). Inbred strains (A/J, DBA/2J, and C57BL/6J) were compared by one-way ANOVA (P = 0.0039) with post-hoc Tukey HSD pairwise comparisons indicated on graph. **(H)** Example fluorescent image of an A/J 7-day post-MI heart fixed in 4% paraformaldehyde, embedded in paraffin, sectioned at 4 uM, and stained for anti-NKX2–5 (red), anti-Aurora Kinase B (AURKB, green), cardiac troponin T (cTnT, magenta), and DAPI (greyscale). **(I)** Quantification of green AURKB puncta residing distinctly between two adjacent CMs (as in H) across sections of infarcted myocardium. N=3 A/J and 3 C57BL/6J 7-days post-MI. P-value assessed by unpaired Student's T-test. **(J)** Total EdU^+ CMs (Log2 scale) identified in single-cell suspensions of ventricular tissue post-infarction in *Tnni3k* wild-type (*Tnni3k* +/+) and *Tnni3k* knockout (*Tnni3k* −/−) littermates, N addressed above in (A). The *Tnni3k* knockout line has been maintained on a C57BL/6J inbred background. P-value assessed by unpaired Student's T-test. **(K)** Percent of EdU^+ CMs from post-MI single-cell suspensions that were specifically mononuclear and diploid represented as a percent of the total EdU^+ CM population comparing *Tnni3k* +/+ and *Tnni3k* −/− littermates. P-value assessed by unpaired, one-tailed Student's T-test with Welch's correction for unequal variance.